An S-Type Anion Channel SLAC1 Is Involved in Cryptogein-Induced Ion Fluxes and Modulates Hypersensitive Responses in Tobacco BY-2 Cells

Takamitsu Kurusu[1,2,3][9], Katsunori Saito[1][9], Sonoko Horikoshi[1], Shigeru Hanamata[1], Juntaro Negi[4], Chikako Yagi[1], Nobutaka Kitahata[1], Koh Iba[4], Kazuyuki Kuchitsu[1,2]*

1 Department of Applied Biological Science, Tokyo University of Science, Noda, Chiba, Japan, 2 Research Institute for Science and Technology, Tokyo University of Science, Noda, Chiba, Japan, 3 School of Bioscience and Biotechnology, Tokyo University of Technology, Hachioji, Tokyo, Japan, 4 Department of Biology, Faculty of Science, Kyushu University, Fukuoka, Japan

Abstract

Pharmacological evidence suggests that anion channel-mediated plasma membrane anion effluxes are crucial in early defense signaling to induce immune responses and hypersensitive cell death in plants. However, their molecular bases and regulation remain largely unknown. We overexpressed Arabidopsis *SLAC1*, an S-type anion channel involved in stomatal closure, in cultured tobacco BY-2 cells and analyzed the effect on cryptogein-induced defense responses including fluxes of Cl^- and other ions, production of reactive oxygen species (ROS), gene expression and hypersensitive responses. The SLAC1-GFP fusion protein was localized at the plasma membrane in BY-2 cells. Overexpression of *SLAC1* enhanced cryptogein-induced Cl^- efflux and extracellular alkalinization as well as rapid/transient and slow/prolonged phases of NADPH oxidase-mediated ROS production, which was suppressed by an anion channel inhibitor, DIDS. The overexpressor also showed enhanced sensitivity to cryptogein to induce downstream immune responses, including the induction of defense marker genes and the hypersensitive cell death. These results suggest that SLAC1 expressed in BY-2 cells mediates cryptogein-induced plasma membrane Cl^- efflux to positively modulate the elicitor-triggered activation of other ion fluxes, ROS as well as a wide range of defense signaling pathways. These findings shed light on the possible involvement of the SLAC/SLAH family anion channels in cryptogein signaling to trigger the plasma membrane ion channel cascade in the plant defense signal transduction network.

Introduction

Plants respond to pathogen attacks by activating a variety of immune responses, which restrict pathogen growth at the site of infection [1]. These responses are initiated by recognition of signal molecules/elicitors derived from microbes/pathogens or damaged plant tissues [2].

Upon recognition of the signals, plant cells activate a widespread signal transduction network involving second messengers to trigger inducible immune responses. Characteristic early signaling events include membrane depolarization, plasma membrane effluxes of anions and K+, cytosolic Ca2+ rise, pH changes (cytosolic acidification/extracellular alkalinization), production of reactive oxygen species (ROS), and activation of the mitogen-activated protein kinase (MAPK) cascade [3–9]. These initial responses are followed by the synthesis of phytoalexins, vacuolar collapse, hypersensitive cell death, and activation of pathogenesis-related (PR) genes [10–12]. These downstream events are often prevented when anion release through the plasma membrane is

compromised by several anion channel blockers [13,14], suggesting the importance of anion release through the plasma membrane in the induction of these responses. Indeed, several studies have reported that in various types of mammalian cells, activation of plasma membrane Cl^- channels is an early prerequisite to apoptotic events including cell shrinkage, cytochrome c release, and programmed cell death [15,16]. These results highlight the involvement of anion release mediated by anion channels located on the plasma membrane in early defense signaling processes. However, the molecular bases for the anion effluxes and its regulation in immune responses remain largely unknown.

Several types of anion channels differing in their voltage dependence, kinetic properties, and anion selectivity have been characterized, mostly by electrophysiological techniques in plants [17–19]. Recently, molecular and electrophysiological studies have shown that Arabidopsis SLAC1 is required for anion channel activity in the plasma membrane of guard cells and are more permeable to Cl^- than malate [17], indicating that SLAC1 functions as a slow-type (S-type) anion channel located at the

plasma membrane. This channel, activated by the stress hormone abscisic acid (ABA), ozone, and CO_2, is involved in the early steps leading to stomatal closure [20–22]. Four orthologs of *SLAC1*, *SLAH1-4* have been identified in Arabidopsis, which constitute the SLAC/SLAH family [20]. However, physiological roles of any SLAC/SLAH family proteins in plant immunity remain totally unknown.

Cryptogein, a 10-kDa proteinaceous elicitor produced by the pathogenic oomycete *Phytophthora cryptogea*, induces a variety of immune responses such as membrane potential changes, extra-cellular alkalinization, ion fluxes including Ca2+, production of ROS and nitric oxide, MAPK activation, defense-related gene expression, and induction of hypersensitive cell death accompanied by vacuolar collapse in tobacco plants and suspension-cultured cells [4,11,23–26]. Recent transcriptomic and proteomic analyses have revealed many components involved in the cryptogein signaling network in tobacco [27,28]. Cryptogein also triggers anion efflux, and pharmacological analyses with anion channel inhibitors including DIDS, 4,4′-diisothiocyanostilbene-2,2′-disulfonic acid, suggest importance of the anion efflux mediated by the plasma membrane anion channels in induction of cryptogein-induced responses in tobacco BY-2 cells [4]. Cryptogein signaling in BY-2 cells thus provide an excellent model system for understanding the roles of anion channels in plant immunity.

We here investigated the effects of overexpression of Arabidopsis SLAC1, an S-type anion channel, on various cryptogein-induced responses in BY-2 cells. SLAC1 expression enormously enhanced cryptogein-induced hypersensitive responses, such as ion fluxes, ROS production, defense-related gene expression, and hypersensitive cell death. Possible physiological function of the SLAC/SLAH family anion channels is discussed.

Materials and Methods

Plant material, transformation and selection of transformed cell lines, and growth conditions

The tobacco BY-2 (*Nicotiana tabacum* L. cv. Bright Yellow-2) cell suspension was grown in modified Linsmaier and Skoog (LS) medium as reported [29], and agitated on a rotary shaker at 100 rpm at 25°C in the dark and used 1 week after subculture. To overexpress *SLAC1* in both BY-2 cells, *SLAC1* cDNA [20] was cloned into a Ti-based vector pBI121 downstream of a CaMV *35S* promoter.

Transformation of BY-2 cells was carried out as described in [30] with minor modifications as follows: 4 ml of 3-day-old exponentially growing culture was transferred to a 90 mm Petri dish and incubated at 28°C with 100 µl of fresh overnight-culture of *Agrobacterium tumefaciens* pGV2260 containing the binary vector pBI121. After 48-h co-cultivation, tobacco cells were washed and plated onto LS agar medium containing kanamycin (100 µg ml^{-1}) and claforan (100 µg ml^{-1}) (Sanofi Aventis Co., Tokyo, Japan). Every 3 to 4 weeks, transformants were selected and transferred onto fresh medium for continued selection.

Chemicals

DIDS and FM4-64 were obtained from Life technologies (Carlsbad, CA, USA). DPI (diphenylene iodonium), K-252a, and luminol were purchased from Wako Pure Chemical (Osaka, Japan).

Expression and purification of cryptogein

Pichia pastoris (strain GS115) carrying the plasmid pLEP3 was used for cryptogein production [4]. Cryptogein was produced

according to O′Donohue et al. [31] and was dissolved in distilled water. Cryptogein concentration was determined using UV spectroscopy employing extinction coefficients of 8306 M^{-1}cm^{-1} at 277 nm [32].

Measurement of pH and [Cl$^-$]

To monitor pH of the culture medium, aliquots of cells (30 g fresh weight) that had been subcultured for 3 d were transferred to 30 ml of fresh culture medium lacking KH$_2$PO$_4$. For extracellular Cl$^-$ concentration, aliquots of cells (30 g fresh weight) that had been subcultured for 7 d were transferred to 30 ml of fresh culture medium replacing CaCl$_2$ with CaSO$_4$. After a 3 h equilibration period on a gyratory shaker (160 rpm, 25°C) in open 100-ml vials, the pH of the culture medium was measured by the compact pH meter (Model AS-212, Horiba, Kyoto, Japan) according to the manufacturer's protocol. [Cl$^-$] of the culture medium was measured with a pH/Ion meter (Model F-53, Horiba) with a combination electrode sensitive to Cl$^-$ (Model 8002, Horiba).

Measurement of H$_2$O$_2$ in tobacco BY-2 cells

BY-2 cells (3 day after subculture) were used for the ROS production assay. To monitor initial H$_2$O$_2$, cells were washed and resuspended in 5 mM MES buffer (pH 8.0) containing 175 mM mannitol, 0.5 mM CaCl$_2$, and 0.5 mM K$_2$SO$_4$. After a 3 h equilibration period on a gyratory shaker (160 rpm, 25°C), 0.462 mM luminol and 5 mM Tris buffer (pH 8.0) was added. Fifteen minutes after luminol application, H$_2$O$_2$-dependent chemiluminescence was monitored with a luminometer (Lumi-counter 2500, Microtech Nition, Chiba, Japan), in which the culture tube rotates 17 revolutions every 3 s clockwise and counterclockwise in turn, and agitates the cells [4].

To detect prolonged H$_2$O$_2$ production, an aliquot (25 µl) of medium was mixed in a 96-well microtiter plate with 150 µl 50 mM Tris-HCl (pH 8.0) and 25 µl 0.462 mM luminol in 50 mM Tris-HCl, pH 8.0. Potassium ferricyanide (25 µl, 11.76 mM) was added, and H$_2$O$_2$-dependent chemiluminescence was recorded for 15 s using a luminometer (MicroLumat Plus LB96V, Berthold Technologies, Bad Wildbad, Germany).

To quantify the effects of inhibitors on ROS production, the peak intensity of luminol chemiluminescence was compared and relative luminescence levels in the control were standardized as 100%.

Cell death assay with Evans blue

An aliquot of the cell suspension (50 mg fresh weight in 0.5 ml) was incubated with 0.05% Evans blue (Sigma, St. Louis, MO, USA) for 10 min and washed to remove unabsorbed dye. The selective staining of dead cells with Evans blue depends on extrusion of the dye from living cells via an intact plasma membrane [33]. Cell death was quantified by counting stained cells (250–300 cells per each treatment) using a microscope.

MTT reductase activity

An aliquot of the cell suspension (50 mg fresh weight in 0.5 ml) was incubated with 0.2 ml of 12 mM MTT (3-(4, 5-dimethyl-2-thiazolyl)-2, 5-diphenyl-2H tetrazolium bromide) solution (DO-JINDO, Tokyo, Japan) for 0.5 h at 28°C. The supernatant was removed by centrifugation and 1 ml of acidic isopropanol (40 mM HCl) was added to stained cells, followed by incubation at 60°C for 15 min to elute the dye from the cells. A_{595} was measured to measure the reductase activity.

Reverse transcriptase (RT)-PCR analysis

Total RNA was isolated using Sepasol (Nacalai tesque, Kyoto, Japan) according to the manufacturer's protocol and quantified with a spectrophotometer. First-strand cDNA was synthesized from 3 μg total RNA with an oligo-dT primer (Life technologies) and reverse transcriptase (Promega, Fitchburg, WI, USA). PCR amplification was performed with an initial denaturation at 95°C for 3 min followed by the indicated number of cycles of incubations at 94°C for 30 s, 55°C for 90 s, and 72°C for 1 min, and a final extension at 72°C for 10 min using Arabidopsis SLAC1-specific primers (SLAC1-F 5′-GCCATTAGCG-TACCTCCCAT-3′, SLAC1-R 5′- GCAGATATTTTCTTCGC-CAG-3′). EF-1α (EF1α-F 5′-ATTCAAG-TATGCCTGGGTGCTTGAC-3′, EF1α-R 5′-TTCGTTGTCGAGGACCATGC-3′) was used as a quantitative control. Aliquots of individual PCR products were resolved by agarose gel electrophoresis and visualized by ethidium bromide staining using a UV light.

Real-time RT-PCR quantification

Real-time RT-PCR assays were performed as described by Kurusu et al. [34]. First-strand cDNA was synthesized from 2 μg of total RNA using an oligo-dT primer (Life technologies) and reverse transcriptase (Promega). Real-time PCR was performed using an ABI PRISM 7300 sequence detection system (Life technologies) with THUNDERBIRD SYBR qPCR Mix (TOYOBO, Osaka, Japan) and gene specific primers. The following PCR primers were used: Hsr203j-RealF, 5′-GTCTTATCGGAGCAAATCGGAGTTAG-3′; Hsr203j-RealR, 5′-CTCCCATCGGACATGTTATTGG-3′; HIN1-RealF, 5′-GAGGGTCACAAGAATACTAGCAGC-3′; HIN1-RealR, 5′-CGCATGTAAAGCTTCACTTCCATCTC-3′; NtRbohD-RealF, 5′-GCGGCAAGTCCAATGATGA-3′; NtRbohD-RealR, 5′-GAATCTTCGCGGACATCGA-3′; NtActin-RealF, 5′-GGGTTTGCTGGAGATGATGCT-3′; NtActin-RealR, 5′-GCTTCATCACCAACATATGCAT-3′ PR1a-RealF, 5′-GTGGGTTAGCGAGAAGGCTA-3′; PR1a-RealR, 5′-ACTTTGGCACATCCGAGTCT-3′; AtTUB2-RealF, 5′-ATTCCCCCGTCTTCACTTCT-3′; AtRbohD-RealF, 5′-CCTCAACAACACCACCTCCT-3′; AtRbohD-RealR, 5′-GTAAGAGGCCGTTGGAATCA-3′; AtTUB2-RealF, 5′-ATTCCCCCGTCTTCACTTCT-3′;AtTUB2-RealR, 5′-CA-CATTCAGCATCTGCTCGT-3′;. Relative mRNA abundances were calculated using the standard curve method and normalized to corresponding NtActin and AtTUB2 gene levels. Standard samples of known template amounts were used to quantify PCR products.

Intracellular localization of GFP fusion proteins

The green fluorescence protein (GFP) sequence derived from sGFP [35] was fused to the C terminus of Arabidopsis SLAC1 cDNA and was cloned into a transient assay vector pUC19 downstream of a CaMV 35S promoter. The original sGFP plasmid was used as a control. Protoplasts were prepared from 3 d BY-2 cells using a standard method [29], and plasmids were introduced into BY-2 protoplasts by polyethylene glycol-mediated transformation [36]. One day after transformation, GFP fluorescence images were observed using a LSM 5 EXCITER confocal fluorescence microscope with a C-Apochromat 40×/1.2W corr (water) (Carl Zeiss, Oberkochen, Germany) as an objective lens. Images were processed using the Zeiss LSM Image Browser (Carl Zeiss Inc.) and the Adobe Photoshop Element 7.0 (Adobe Systems, San Jose, CA, USA).

Statistical analysis

Statistical significance was determined using an unpaired Student's t test; $P < 0.05$ indicated significance.

Accession numbers of the genes

The accession numbers for the genes described are as follows: SLAC1 (At1g12480), SLAH1 (At1g62280), SLAH2 (At4g27970), SLAH3 (At5g24030), SLAH4 (At1g62262), HIN1 (AB091429), Hsr203j (X77136), NtRbohD (AF506374), OST1 (At4g33950), CPK21 (At4g04720), CPK23 (At4g04740), PR1a (At2g14610), AtRbohD (At5g47910).

Results

Involvement of anion channels on cryptogein-induced hypersensitive responses in BY-2 cells

Pharmacological evidence suggests the importance of anion channel-mediated anion efflux in cryptogein-induced initial responses in cultured tobacco cells [14]. We therefore checked the effect of an anion channel inhibitor, DIDS, on cryptogein-induced hypersensitive responses in BY-2 cells.

Increasing evidence suggests the involvement of mitochondrial dysfunction in the induction of hypersensitive cell death in plants as well as in animals [37]. MTT reductase activity was monitored as a marker for mitochondrial function [10]. As shown in Fig. 1A, cryptogein induced a rapid reduction in MTT reductase activity in BY-2 cells in a time-dependent manner, which was significantly inhibited by DIDS (Fig. 1B). A Ser/Thr protein kinase inhibitor, K-252a also suppressed the reduction in MTT reductase activity in a dose-dependent manner (Fig. S1).
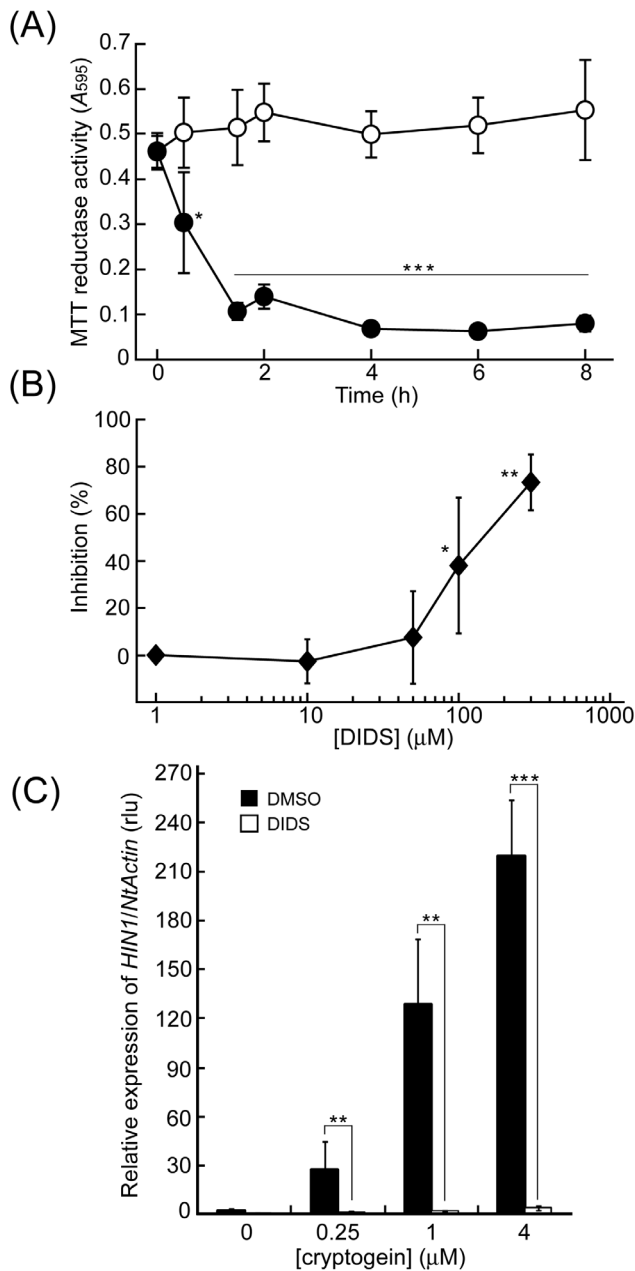
The expression of a harpin-induced gene HIN1 has been suggested to correlate with hypersensitive responses [38]. The expression of HIN1 was induced 5 h after the application of cryptogein (Fig. 1C), which was strongly reduced by DIDS (Fig. 1C). These results suggest that anion channels are involved in the regulation of cryptogein-induced hypersensitive responses in BY-2 cells.

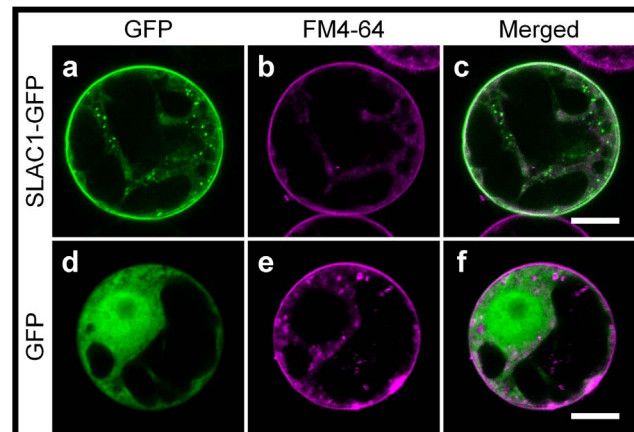## Intracellular localization of the SLAC1 protein in BY-2 cells

Arabidopsis SLAC1 is an S-type anion channel located at the plasma membrane in guard cells [20,22]. To study intracellular localization of the SLAC1 protein expressed in BY-2 cells, we introduced the GFP construct fused to the C-terminus of SLAC1 into BY-2 protoplasts and examined its intracellular localization by confocal laser scanning microscopy. When GFP alone was expressed, it localized to the nucleus and the cytoplasm (Fig. 2; d-f). In contrast, the SLAC1-GFP fusion protein was specifically targeted to the plasma membrane; fluorescent images of SLAC1-GFP were clearly different from those of FM4-64, a marker for internal membranes (Fig. 2; a-c), indicating that SLAC1 functions at the plasma membrane in BY-2 cells as in Arabidopsis guard cells.

Effect of SLAC1 overexpression on cryptogein-induced ion fluxes

To test possible involvement of SLAC1 in the cryptogein-induced plasma membrane anion efflux, we generated transgenic tobacco BY-2 cell lines expressing Arabidopsis SLAC1 by means of Agrobacterium-mediated transformation [30]. Several transformant lines were obtained and the expression of SLAC1 mRNA in BY-2 cells was confirmed by RT-PCR analyses (Fig. S2). Finally, four

Figure 2. Intracellular localization of the SLAC1 protein in tobacco BY-2 cells. Confocal fluorescence images (**a-f**) of BY-2 protoplast expressing SLAC1-GFP (**a–c**) or GFP (**d–f**) stained with the fluorescent styryl membrane probe FM4-64. Fluorescence of GFP (**a** and **d**) and FM4-64 (**b** and **e**). Scale bar: 10 μm. FM4-64 was kept as a 17 mM stock solution in sterile water, and used at a final concentration of 4.25 μM. Tobacco BY-2 protoplasts were treated with FM4-64 for 10 min and washed twice with the wash buffer at room temperature to label the PM.
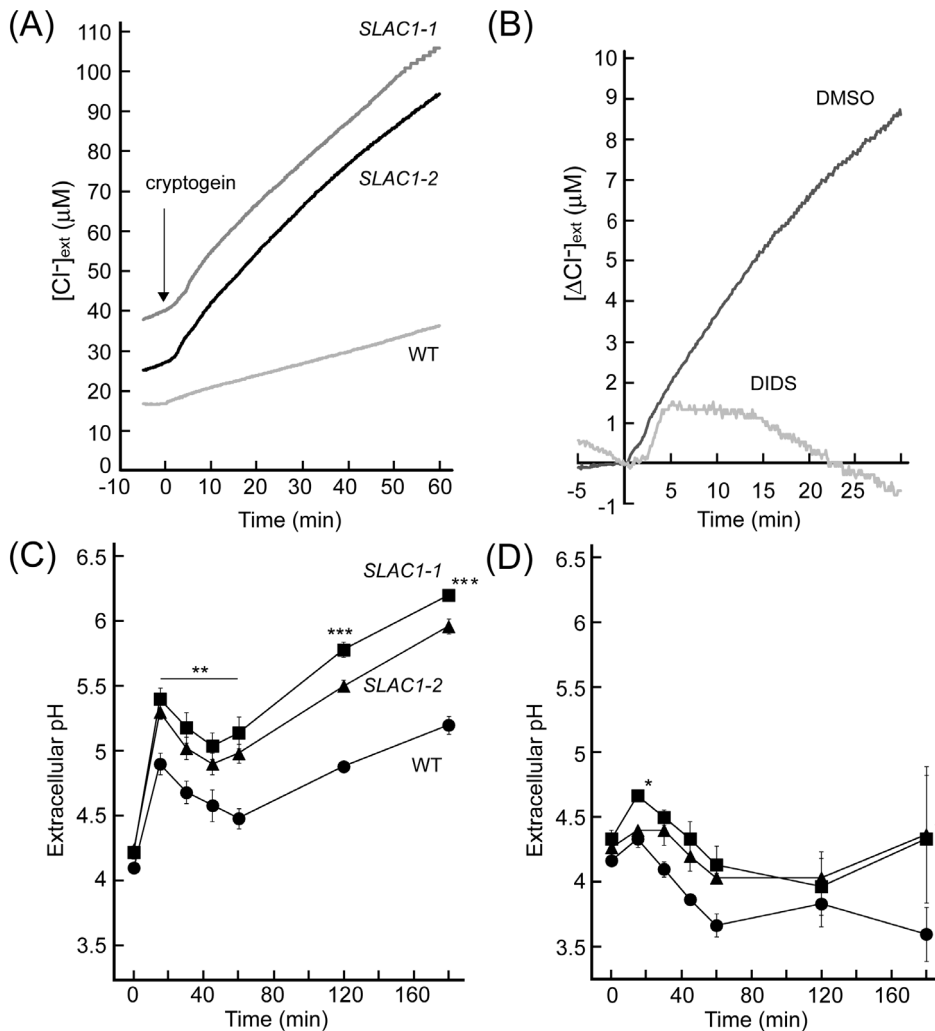doi:10.1371/journal.pone.0070623.g002

transformant lines (line No. 1–4) were selected for further investigation.

To confirm if SLAC1 plays a role in anion transport in BY-2 cells, we tested whether the expression levels of *SLAC1* mRNA affected anion transport activity. Extracellular Cl^- concentration ($[Cl^-]_{ext}$) was simultaneously monitored with ion-selective electrodes in the growth medium. Extracellular $[Cl^-]$ showed a prolonged increase after cryptogein application (Fig. 3A), which is consistent with our previous report [4]. As shown in Fig. 3A, cryptogein-induced Cl^- efflux was significantly higher in the *SLAC1*-overexpressing cells than in non-transgenic control cells. DIDS clearly suppressed cryptogein-induced Cl^- efflux (Figs. 3B), suggesting that an S-type anion channel, SLAC1, is involved in the cryptogein-induced plasma membrane Cl^- efflux in BY-2 cells.

Pharmacological evidence suggests the importance of Cl- efflux in cryptogein-induced initial signaling events in BY-2 cells [4,13]. Since SLAC1 has been suggested to be involved in the regulation of Cl- efflux (Fig. 3A, B), we investigated possible involvement of SLAC1 in cryptogein-induced pH change as a marker for the initial plasma membrane signaling events [4]. Cryptogein induced biphasic slow and prolonged extracellular alkalinization (Fig. 3C), which is consistent with our previous report [4]. This elicitor–induced extracellular alkalinization was much more evident in *SLAC1* overexpressors than in non-transgenic control cells, which were severely inhibited by DIDS (Fig. 3C, D). These results suggest that SLAC1-mediated Cl- efflux modulates other ion fluxes known as initial defense signaling events in BY-2 cells.

Involvement of SLAC1 in the regulation of cryptogein-induced biphasic ROS production

Production of hydrogen peroxide (H_2O_2) was monitored by an assay using luminol chemiluminescence [39]. As shown in Fig. 4A, cryptogein triggered rapid ROS production within 5 min, which is consistent with our previous report [4]. The increment of ROS production was dramatically enhanced in the *SLAC1* over-expressors than the control at a low concentration of cryptogein (Fig. 4A). An NADPH oxidase inhibitor, DPI (10 μM), almost completely abolished cryptogein-induced ROS production both in

Figure 1. Effect of DIDS on cryptogein-induced mitochondrial dysfunction and expression of *HIN1* in BY-2 cells. (A) Cryptogein (1 μM)-induced reductions in MTT reductase activity. MTT reductase activity was used as a putative marker for mitochondrial dysfunction. Black circle: cryptogein treatment, white circle: water treatment as a control. *** *p*<0.001, significantly different from the control. (B) Inhibitory effect of DIDS on cryptogein-induced reductions in MTT reductase activity. BY-2 cells 3 h after the addition of the cryptogein elicitor (1 μM). DIDS or DMSO was added to BY-2 cells 15 min prior to the elicitor treatment. Data are the mean ± SE of three independent experiments. * *p*<0.05, ** *p*<0.005, significantly different from the control. DMSO was used as a control. (C) Effect of DIDS on cryptogein-induced *HIN1* expression. Total RNA was isolated from BY-2 cells harvested 2 h after the addition of cryptogein. DIDS (white bars) or DMSO (black bars) was added to BY-2 cells 15 min prior to the elicitor treatment. The amount of each mRNA was calculated from the threshold point located in the log-linear range of RT-PCR. The relative level of each gene in control cells at time 0 was standardized as 1. Data are the mean ± SE of three independent experiments. ** *p*<0.005, *** *p*<0.001, significantly different from the control.
doi:10.1371/journal.pone.0070623.g001

Figure 3. Effect of *SLAC1*-overexpression on cryptogein-induced ion fluxes. (A) Time course of cryptogein-induced [Cl⁻]$_{ext}$ changes in BY-2 cells. BY-2 cells were treated with cryptogein (0.25 μM). (B) Effect of DIDS on cryptogein-induced [Cl⁻]$_{ext}$ changes. DIDS (100 μM) was added to BY-2 cells 15 min prior to the elicitor (0.25 μM) treatment. DMSO was used as a control. (C) Time course of cryptogein-induced [pH]$_{ext}$ changes. BY-2 cells were treated with cryptogein (1 μM). ** $p<0.005$, *** $p<0.001$, significantly different from the control line. (D) Effect of DIDS on cryptogein-induced [pH]$_{ext}$ changes. DIDS (50 μM) was added to BY-2 cells 15 min prior to the elicitor treatment. DMSO was used as a control. Data are the mean ± SE of three independent experiments. * $p<0.05$, significantly different from the control line.
doi:10.1371/journal.pone.0070623.g003

SLAC1-overexpressors and the control (Fig. 4B), suggesting that cryptogein-triggered ROS production is predominantly mediated by NADPH oxidases [4]. DIDS clearly suppressed elicitor-induced ROS production (Fig. 4B), suggesting that overexpression of *SLAC1* leads to enhanced activation of the NADPH oxidases. Taken together, SLAC1-mediated anion efflux is suggested to affect the regulation of NADPH-oxidase activity.
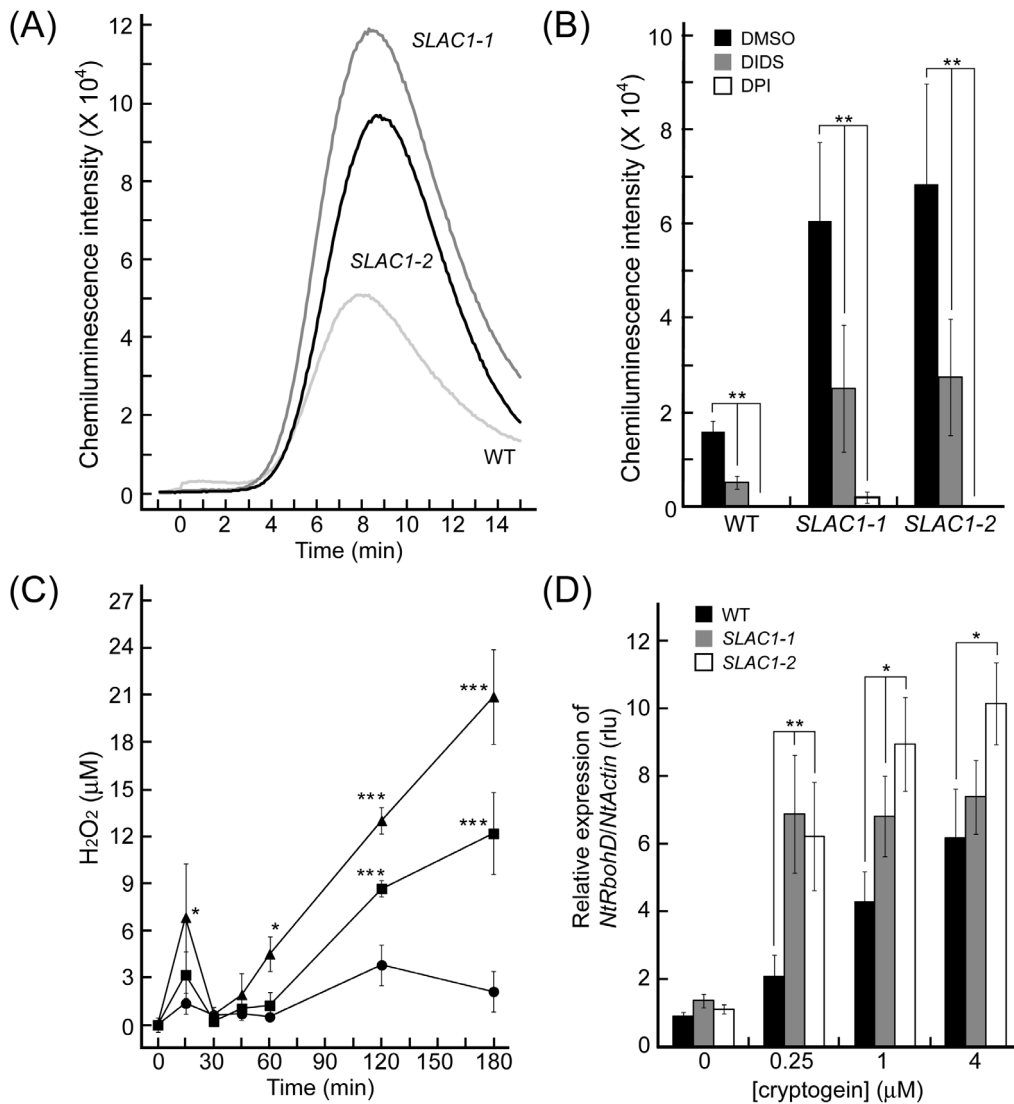
Cryptogein induces biphasic (rapid/transient and slow/prolonged) ROS production in tobacco BY-2 cells [40]. Expression of a tobacco NOX homolog *NtRbohD*, encoding NADPH oxidase, is induced in response to cryptogein/elicitors or avirulent pathogens and is suggested to be essential for the slow and prolonged ROS production [40–43]. As shown in Fig. 4C and D, the time course of cryptogein-induced prolonged ROS production and expression of *NtRbohD* correlated well, and both of them were significantly enhanced in the *SLAC1*-overexpressors in comparison with the control at a low concentration of cryptogein. DIDS severely inhibited cryptogein-induced prolonged ROS production (data not shown) as the rapid/transient ROS production (Fig. 4B). Taken

together, these results suggest that SLAC1-mediated anion flux is involved in the regulation of cryptogein-induced expression of respiratory burst oxidase homologs (Rbohs) and NADPH oxidase-mediated ROS production.

Involvement of SLAC1 in the regulation of cryptogein-induced defense gene expression and hypersensitive cell death

Rbohs have been suggested to be involved in ROS production and the regulation of hypersensitive cell death in Arabidopsis and rice [44–46]. To further characterize the role of SLAC1 in the downstream signaling pathway elicited by cryptogein, we analyzed the induction of defense-related genes and hypersensitive cell death in the *SLAC1*-overexpressors.

Hypersensitive-related (*hsr*) gene, *Hsr203J*, that encodes a serine hydrolase with esterase activity, is postulated to regulate either the establishment or limitation of cell death [47]. The expression of *HIN1* is correlated with hypersensitive responses [38]. The

Figure 4. Involvement of SLAC1 in the regulation of cryptogein-induced biphasic ROS production mediated by NADPH oxidases.
(A) Cryptogein (0.25 µM)-induced rapid transient ROS production within 15 min in BY-2 cells. Data is representative of three experiments (B) The effects of inhibitors on cryptogein-induced ROS production within 15 min. To quantify the effects of inhibitors on ROS production, the peak intensity of luminol chemiluminescence was compared with the control. DIDS or an NADPH oxidase inhibitor, DPI, was added to BY-2 cells 15 min prior to the elicitor treatment. DMSO was used as a control. Data are the mean ± SE of three independent experiments. ** $p<0.005$, significantly different from the control line. (C) Effect of SLAC1-overexpression on cryptogein-induced prolonged ROS production. BY-2 cells were treated with cryptogein (0.25 µM). Data are the mean ± SE of three independent experiments. * $p<0.05$, ** $p<0.005$, *** $p<0.001$, significantly different from the control line. (D) Quantitative expression levels of NtRbohD mRNAs in SLAC1-overexpressing cells by real-time quantitative PCR. Total RNA was isolated from BY-2 cells harvested 5 h after the addition of cryptogein at various concentrations. The amount of each mRNA was calculated from the threshold point located in the log-linear range of the RT-PCR. The relative level of each gene in the control cells at time 0. Data are the mean ± SE of four independent experiments. * $p<0.005$, ** $p<0.005$, significantly different from the control line.
doi:10.1371/journal.pone.0070623.g004

expression of *HIN1* and *Hsr203J* were induced 5 h after the application of cryptogein in non-transgenic cells (Fig. 5A, B). At lower concentration range of the elicitor, the expression of both *HIN1* and *Hsr203J* were significantly higher in the *SLAC1*-overexpressors than in the control. At higher concentrations of cryptogein (4 µM), the expression of the genes was almost comparable between the overexpressors and the control (Fig. 5A, B).

Hypersensitive cell death as a form of programmed cell death is a crucial event to prevent the spread of biotrophic pathogens [12]. Anion efflux has been suggested to be involved in the regulation of cryptogein-induced hypersensitive cell death in cultured tobacco

cells [14]. Evans blue staining was applied to quantify the levels of cell death [40]. As shown in Fig. 6, hypersensitive cell death was much more evident in the *SLAC1*-overexpressors than that of the control cells, and the levels of cell death corresponded with the expression levels of *SLAC1*. Overall, these results indicate that the overexpression of *SLAC1* led to enhance the sensitivity to cryptogein to induce hypersensitive cell death.
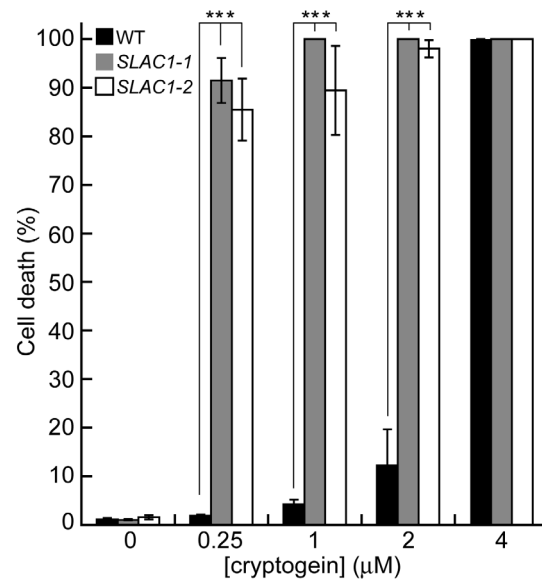
Discussion

Anion efflux has been suggested to play crucial roles in plant defense responses [4,13,14,48]. However, the molecular bases for
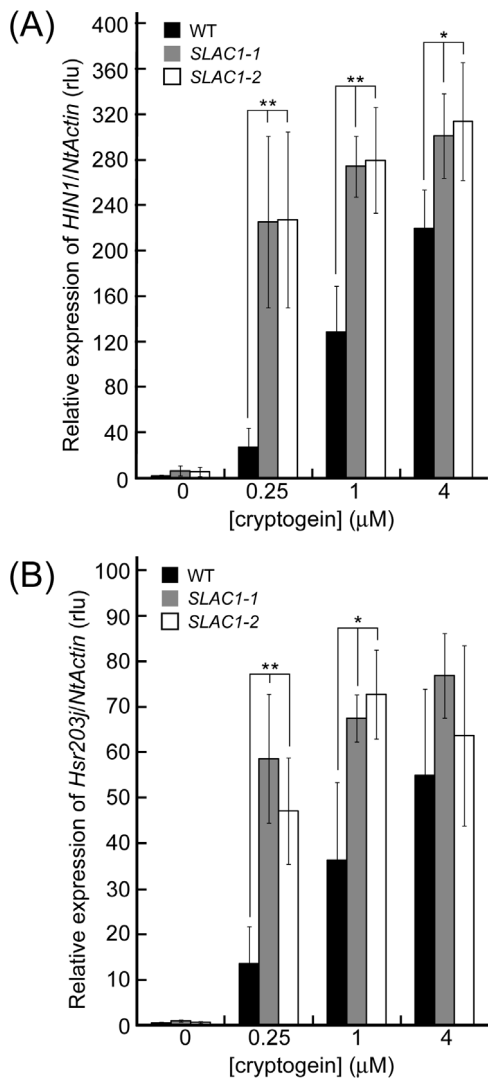
Figure 5. Effect of *SLAC1*-overexpression on cryptogein-induced defense gene expressions. (A and B) Cryptogein-induced the expression of *HIN1* in a dose-dependent manner (A) and *Hsr203j* (B) in *SLAC1*-overexpressing cells. The amount of each mRNA was calculated from the threshold point located in the log-linear range of the RT-PCR. The relative level of each gene in the control cells at time 0. Total RNA was isolated from BY-2 cells harvested 5 h after the addition of cryptogein at various concentrations. Data are the mean ± SE of three independent experiments. * $p < 0.05$, ** $p < 0.005$, significantly different from the control line.
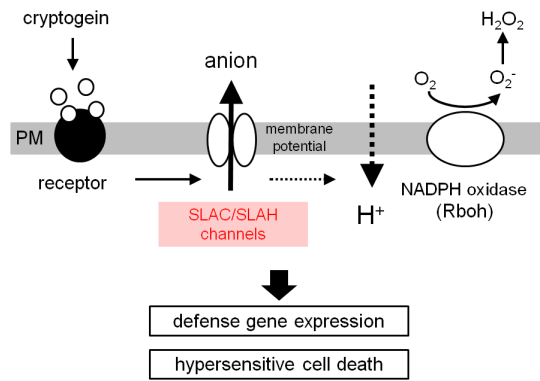doi:10.1371/journal.pone.0070623.g005

Figure 6. Effect of *SLAC1*-overexpression on cryptogein-induced hypersensitive cell death. Cryptogein-induced cell death in a dose-dependent manner in *SLAC1*-overexpressing cells. BY-2 cells 24 h after the addition of the cryptogein elicitor at various concentrations. Evans blue staining was applied to quantify the level of cryptogein-induced cell death. Data are the mean ± SE of five independent experiments. **** $p < 0.001$, significantly different from the control line.
doi:10.1371/journal.pone.0070623.g006

(Figs. 1A and 6), suggesting the possible involvement of mitochondrial dysfunction on the induction/regulation of the programmed cell death.

The present results indicate that cryptogein-induced mitochondrial dysfunction requires the plasma membrane anion effluxes and protein phosphorylation (Figs. 1B and S1). The anion channel activity of SLAC1 is regulated by protein phosphorylation and has been suggested to be phosphorylated by several protein kinases, such as OST1, CPK21, and CPK23, which are key regulators in the stomatal movement of Arabidopsis guard cells [49–52]. Recently, some Ca2+-regulated protein kinases, such as calcium-dependent protein kinases (CDPK/CPK) and CBL-interacting protein kinases (CIPK), have been shown to be involved in the regulation of a variety of immune responses including initial events in many plant species [10,53,54]. SLAC/SLAH family anion channels may be phosphorylated by some of these protein kinases, and the phosphorylation may be involved in the activation of elicitor-triggered anion effluxes to regulate the induction of mitochondria-mediated hypersensitive cell death.

SLAC1-mediated anion efflux plays a key role in the stomatal closure elicited by environmental stimuli, such as ABA, ozone, and CO2 in Arabidopsis guard cells [20–22]. However, the interrelationship among SLAC1-mediated anion efflux, transcriptional regulation of a variety of genes and ROS production as important signalling events to transmit precise initial responses to downstream pathways remain mostly unknown. We here showed that the overexpression of *SLAC1* enhanced cryptogein-induced expression of defense-related genes and *NtRbohD*, which is involved in the enzymatic ROS production (Figs. 4D and 5). Cryptogein-induced *HIN1* expression was severely inhibited by an anion channel blocker, DIDS (Fig. 1C), indicating that expression of these genes are regulated by cryptogein-induced SLAC1-mediated plasma membrane anion efflux. Anion channel-mediated anion

anion efflux and its regulation in immune responses remain largely unknown. The present functional characterization of the *SLAC1* overexpressors and pharmacological analyses suggest that an S-type anion channel, SLAC1, is specifically activated in response to cryptogein, and involved in the regulation of cryptogein-induced Cl⁻ efflux across the plasma membrane, defense-related gene expression, induction of hypersensitive cell death as well as NADPH oxidase-mediated biphasic ROS production in BY-2 cells.

Increasing evidence suggests the importance of mitochondria in the induction of hypersensitive cell death in defense signaling pathways [10]. We here showed that cryptogein triggered reduction in the mitochondrial reductase activity prior to the induction of hypersensitive cell death in tobacco BY-2 cells

Figure 7. A hypothetical model for cryptogein-induced anion efflux, ROS production and hypersensitive response in tobacco BY-2 cells. Unbroken and broken arrows indicate established and hypothetical links, respectively.
doi:10.1371/journal.pone.0070623.g007

efflux is one of the key factors in membrane depolarization, which may affect gene expression and plant immunity [55].

The present results suggest that SLAC1-mediated anion efflux is activated by cryptogein and positively modulates cryptogein-triggered NADPH oxidase/Rboh-mediated biphasic ROS production (Fig. 4D) as well as hypersensitive cell death (Fig. 6). Rboh-mediated ROS production has been suggested to be involved in the regulation of hypersensitive cell death [44–46]. SLAC1-mediated anion efflux activated by cryptogein may act upstream of activation of Rbohs to regulate downstream defense responses including the programmed cell death.

The cryptogein-induced rapid/transient ROS production within minutes mediated by NADPH oxidase [4] was dramatically enhanced in the *SLAC1*-overexpressors than the control (Fig. 4A, B). Interestingly, the basal expression level of *NtRbohD* and the basal ROS level before the elicitation in the *SLAC1* overexpressors were comparable to those in the control (Fig. 4A, D), suggesting that overexpression of *SLAC1* may lead to enhanced activation of NADPH oxidases by its posttranslational regulation. Rbohs are synergistically activated by direct binding of Ca2+ to their EF-hand regions and phosphorylation mediated by Ca2+−activated protein kinases [53,56–59]. Ca2+ influx or activation of Ca2+−activated protein kinases may be regulated by the plasma membrane potential [60]. Interrelationship among these plasma membrane signaling events mediated by anion efflux should be an important subject for future studies.

To test whether SLAC1 has a role in other defense signaling pathways, we generated the *SLAC1*-overexpressing plants (Fig. S3) and investigated the responses triggered by flg22, a typical microbe/pathogen-associated molecular pattern (MAMP/PAMP), which does not induce hypersensitive cell death [61]. As shown in Figs. S4 and S5, flg22 induced ROS production and expression of defense marker genes *PR1a* and *AtRbohD* in Arabidopsis seedlings, which were comparable between the control and the *SLAC1*-overexpressor. These results appear to be consistent with the recent report that the membrane potential change triggered by flg22 as well as another typical MAMP, elf18 was not affected by some anion channel inhibitors including DIDS, or by a T-DNA insertional mutation in *SLAC1* or *SLAH3*, a homolog of *SLAC1* expressed in mesophyll cells [60]. The SLAC/SLAH family may not play a major role in the major MAMP signaling pathway in Arabidopsis seedlings.

In stomatal guard cells, the SLAC/SLAH anion channels play a key role as a downstream effector in the cell volume regulation

[19,20,22], which appear to be distinct from their roles in signaling, and thus flg22-induced stomatal closure was impaired in the *slac1* mutant [62]. In Arabidopsis cultured cells, pharmacological analyses suggested that R-type anion channels have key roles in cell death and ROS production triggered by the non-specific plant pathogen *Xanthomonas campestris* [48]. Taken together, roles of various anion channels may vary among cell types and triggering signals/types of plant-pathogen interactions.

Finally, we checked the effect of cryptogein in Arabidopsis seedlings. Unlike tobacco, cryptogein scarcely induced hypersensitive responses including expression of defense marker genes in Arabidopsis (data not shown), which was consistent with a previous report [63]. Overall, the present findings suggest that cryptogein-triggered defense responses in tobacco BY-2 cells provide a unique model system for understanding the roles of S-type anion channels and SLAC/SLAH proteins in hypersensitive responses and plant immunity. The exact correlation between the levels of SLAC/SLAH proteins and the plasma membrane anion efflux remains to be evaluated. Loss-of-function experiments using *Ntslac/slah*-suppressed cell lines should be important to further unveil the roles of the SLAC/SLAH proteins in tobacco cells.

Conclusions

The present study suggests that SLAC/SLAH anion channel(s) is involved in the regulation of the plasma membrane Cl^-/anion efflux to modulate not only the plasma membrane signaling events such as other ion fluxes and NADPH oxidase-mediated ROS production but also the signaling pathway(s) to regulate gene expression and hypersensitive cell death triggered by cryptogein in tobacco BY-2 cells (Fig. 7). These findings shed light on the novel aspects of the roles of SLAC/SLAH anion channels and the defense/immune signaling network in plant cells.

Supporting Information

Figure S1 Effect of a Ser/Thr protein kinase inhibitor, K-252a, on cryptogein-induced mitochondrial dysfunction in tobacco BY-2 cells. Cells 3 h after the addition of the cryptogein (1 μM). K-252a or DMSO was added to the cells 15 min prior to the elicitor treatment. Data are the mean ± SE of three independent experiments. ** $p<0.005$, *** $p<0.001$, significantly different from the control. DMSO was used as a control.
(TIF)

Figure S2 Expression levels of *SLAC1* mRNA in 4 independent overexpressing lines of BY-2 cells. First strand cDNA was synthesized from total RNA extracted from each cell lines and amplified indicated cycles by RT-PCR as described in the materials and methods. *EF1α* cDNA was used as a control DNA. PCR products were analyzed by agarose gel electrophoresis.
(TIF)

Figure S3 Expression levels of *SLAC1* mRNA in the overexpressing lines of Arabidopsis. First strand cDNA was synthesized from total RNA extracted from Arabidopsis seedlings and amplified indicated cycles by RT-PCR as described in the materials and methods. *EF1α* cDNA was used as a control. PCR products were analyzed by agarose gel electrophoresis. WT; wild-type (Col-0), OX; *SLAC1*-overexpressor.
(TIF)

Figure S4 Effect of *SLAC1*-overexpression on flg22-induced ROS production in Arabidopsis. Flg22-induced ROS production in a dose-dependent manner in *SLAC1*-

overexpressing Arabidopsis seedlings. Data are the mean ± SE of three independent experiments. The Ws-0 accession of Arabidopsis does not express a functional flg22 receptor [64], and this accession was used as a negative control. Circle; *SLAC1* overexpressor, Square; wild-type (Col-0), Triangle; negative control (Ws-0).
(TIF)

Figure S5 Effect of *SLAC1*-overexpression on flg22-induced gene expressions in Arabidopsis. (A and B) Time course of flg22 (1 µM)-induced the expression of *PR1a* (A) and *AtRbohD* (B) in *SLAC1*-overexpressing Arabidopsis seedlings. The amount of each mRNA was calculated from the threshold point located in the log-linear range of the RT-PCR. The relative level of each gene in the control (Col-0) at time 0. Total RNA was isolated from Arabidopsis seedlings harvested at the indicated times after the addition of flg22. Data are the mean ± SE of three independent experiments.
(TIF)

File S1 Supporting materials & methods.
(DOC)

Author Contributions

Conceived and designed the experiments: TK KK. Performed the experiments: TK KS S. Horikoshi S. Hanamata JN CY NK. Analyzed the data: TK KS S. Horikoshi. Contributed reagents/materials/analysis tools: JN KI. Wrote the paper: TK KK.

References

1. Heath MC (2000) Hypersensitive response-related death. Plant Mol Biol 44: 321–334.
2. Zipfel C (2009) Early molecular events in PAMP-triggered immunity. Curr Opin Plant Biol 12: 414–420.
3. Blume B, Nurnberger T, Nass N, Scheel D (2000) Receptor-mediated increase in cytoplasmic free calcium required for activation of pathogen defense in parsley. Plant Cell 12: 1425–1440.
4. Kadota Y, Goh T, Tomatsu H, Tamauchi R, Higashi K, et al. (2004) Cryptogein-induced initial events in tobacco BY-2 cells: pharmacological characterization of molecular relationship among cytosolic Ca^{2+} transients, anion efflux and production of reactive oxygen species. Plant Cell Physiol 45: 160–170.
5. Kuchitsu K, Kikuyama M, Shibuya N (1993) *N*-acetylchitooligosaccharides, biotic elicitors for phytoalexin production, induce transient membrane depolarization in suspension-cultured rice cells. Protoplasma 174: 79–81.
6. Kuchitsu K, Kosaka H, Shiga T, Shibuya N (1995) EPR evidence for generation of hydroxyl radical triggered by *N*-acetylchitooligosaccharide elicitor and a protein phosphatase inhibitor in suspension-cultured rice cells. Protoplasma 188: 138–142.
7. Kurusu T, Yagala T, Miyao A, Hirochika H, Kuchitsu K (2005) Identification of a putative voltage-gated Ca^{2+} channel as a key regulator of elicitor-induced hypersensitive cell death and mitogen-activated protein kinase activation in rice. Plant J 42: 798–809.
8. Pugin A, Frachisse JM, Tavernier E, Bligny R, Gout E, et al. (1997) Early events induced by the elicitor cryptogein in tobacco cells: Involvement of a plasma membrane NADPH oxidase and activation of glycolysis and the pentose phosphate pathway. Plant Cell 9: 2077–2091.
9. Kikuyama M, Kuchitsu K, Shibuya N (1997) Membrane depolarization induced by *N*-acetylchitooligosaccharide elicitor in suspension-cultured rice cells. Plant Cell Physiol 38: 902–909.
10. Kurusu T, Hamada J, Nokajima H, Kitagawa Y, Kiyoduka M, et al. (2010) Regulation of microbe-associated molecular pattern-induced hypersensitive cell death, phytoalexin production and defense gene expression by calcineurin B-like protein-interacting protein kinases, OsCIPK14/15, in rice cultured cells. Plant Physiol 153: 678–692.
11. Higaki T, Goh T, Hayashi T, Kutsuna N, Kadota Y, et al. (2007) Elicitor-induced cytoskeletal rearrangement relates to vacuolar dynamics and execution of cell death: in vivo imaging of hypersensitive cell death in tobacco BY-2 cells. Plant Cell Physiol 48: 1414–1425.
12. Higaki T, Kurusu T, Hasezawa S, Kuchitsu K (2011) Dynamic intracellular reorganization of cytoskeletons and the vacuole in defense responses and hypersensitive cell death in plants. J Plant Res 124: 315–324.
13. Wendehenne D, Lamotte O, Frachisse JM, Barbier-Brygoo H, Pugin A (2002) Nitrate efflux is an essential component of the cryptogein signaling pathway leading to defense responses and hypersensitive cell death in tobacco. Plant Cell 14: 1937–1951.
14. Gauthier A, Lamotte O, Reboutier D, Bouteau F, Pugin A, et al. (2007) Cryptogein-induced anion effluxes: electrophysiological properties and analysis of the mechanisms through which they contribute to the elicitor-triggered cell death. Plant Signal Behav 2: 86–95.
15. Yu SP, Choi DW (2000) Ions, cell volume, and apoptosis. Proc Natl Acad Sci U S A 97: 9360–9362.
16. Okada Y, Shimizu T, Maeno E, Tanabe S, Wang X, et al. (2006) Volume-sensitive chloride channels involved in apoptotic volume decrease and cell death. J Membr Biol 209: 21–29.
17. Barbier-Brygoo H, De Angeli A, Filleur S, Frachisse JM, Gambale F, et al. (2011) Anion channels/transporters in plants: from molecular bases to regulatory networks. Annu Rev Plant Biol 62: 25–51.
18. Kollist H, Jossier M, Laanemets K, Thomine S (2011) Anion channels in plant cells. FEBS J 278: 4277–4292.
19. Roelfsema MR, Hedrich R, Geiger D (2012) Anion channels: master switches of stress responses. Trends Plant Sci 17: 221–229.
20. Negi J, Matsuda O, Nagasawa T, Oba Y, Takahashi H, et al. (2008) CO_2 regulator SLAC1 and its homologues are essential for anion homeostasis in plant cells. Nature 452: 483–486.
21. Saji S, Bathula S, Kubo A, Tamaoki M, Kanna M, et al. (2008) Disruption of a gene encoding C_4-dicarboxylate transporter-like protein increases ozone sensitivity through deregulation of the stomatal response in *Arabidopsis thaliana*. Plant Cell Physiol 49: 2–10.
22. Vahisalu T, Kollist H, Wang YF, Nishimura N, Chan WY, et al. (2008) SLAC1 is required for plant guard cell S-type anion channel function in stomatal signalling. Nature 452: 487–491.
23. Manzoor H, Chiltz A, Madani S, Vatsa P, Schoefs B, et al. (2012) Calcium signatures and signaling in cytosol and organelles of tobacco cells induced by plant defense elicitors. Cell Calcium 51: 434–444.
24. Garcia-Brugger A, Lamotte O, Vandelle E, Bourque S, Lecourieux D, et al. (2006) Early signaling events induced by elicitors of plant defenses. Mol Plant Microbe Interact 19: 711–724.
25. Vatsa P, Chiltz A, Bourque S, Wendehenne D, Garcia-Brugger A, et al. (2011) Involvement of putative glutamate receptors in plant defence signaling and NO production. Biochimie 93: 2095–2101.
26. Amelot N, Carrouche A, Danoun S, Bourque S, Haiech J, et al. (2011) Cryptogein, a fungal elicitor, remodels the phenylpropanoid metabolism of tobacco cell suspension cultures in a calcium-dependent manner. Plant Cell Environ 34: 149–161.
27. Stanislas T, Bouyssie D, Rossignol M, Vesa S, Fromentin J, et al. (2009) Quantitative proteomics reveals a dynamic association of proteins to detergent-resistant membranes upon elicitor signaling in tobacco. Mol Cell Proteomics 8: 2186–2198.
28. Amelot N, Dorlhac de Borne F, San Clemente H, Mazars C, Grima-Pettenati J, et al. (2012) Transcriptome analysis of tobacco BY-2 cells elicited by cryptogein reveals new potential actors of calcium-dependent and calcium-independent plant defense pathways. Cell Calcium 51: 117–130.
29. Nagata T, Nemoto Y, Hasezawa S (1992) Tobacco by-2 cell-line as the Hela-cell in the cell biology of higher-plants. Inter Review of Cytology-a Survey of Cell Biology 132: 1–30.
30. An GH (1985) High-efficiency transformation of cultured tobacco cells. Plant Physiol 79: 568–570.
31. O'Donohue MJ, Boissy G, Huet JC, Nespoulous C, Brunie S, et al. (1996) Overexpression in *Pichia pastoris* and crystallization of an elicitor protein secreted by the phytopathogenic fungus, *Phytophthora cryptogea*. Protein Expr Purif 8: 254–261.
32. O'Donohue MJ, Gousseau H, Huet JC, Tepfer D, Pernollet JC (1995) Chemical synthesis, expression and mutagenesis of a gene encoding beta-cryptogein, an elicitin produced by *Phytophthora cryptogea*. Plant Mol Biol 27: 577–586.
33. Turner JG, Novacky A (1974) The quantitative relation between plant and bacterial cells involved in the hypersensitive reaction. Phytopathology 64: 885–890.
34. Kurusu T, Yamanaka T, Nakano M, Takiguchi A, Ogasawara Y, et al. (2012) Involvement of the putative Ca^{2+}-permeable mechanosensitive channels, NtMCA1 and NtMCA2, in Ca^{2+} uptake, Ca^{2+}-dependent cell proliferation and mechanical stress-induced gene expression in tobacco (*Nicotiana tabacum*) BY-2 cells. J Plant Res 125: 555–568.
35. Chiu W, Niwa Y, Zeng W, Hirano T, Kobayashi H, et al. (1996) Engineered GFP as a vital reporter in plants. Curr Biol 6: 325–330.
36. Miao Y, Jiang L (2007) Transient expression of fluorescent fusion proteins in protoplasts of suspension cultured cells. Nat Protoc 2: 2348–2353.
37. Lam E, Kato N, Lawton M (2001) Programmed cell death, mitochondria and the plant hypersensitive response. Nature 411: 848–853.

38. Gopalan S, Wei W, He SY (1996) Hrp gene-dependent induction of *hin1*: A plant gene activated rapidly by both harpins and the avrPto gene-mediated signal. Plant J 10: 591–600.

39. Kurusu T, Hamada H, Sugiyama Y, Yagala T, Kadota Y, et al. (2011) Negative feedback regulation of microbe-associated molecular pattern-induced cytosolic Ca^{2+} transients by protein phosphorylation. J Plant Res 124: 415–424.

40. Kadota Y, Fujii S, Ogasawara Y, Maeda Y, Higashi K, et al. (2006) Continuous recognition of the elicitor signal for several hours is prerequisite for induction of cell death and prolonged activation of signaling events in tobacco BY-2 cells. Plant Cell Physiol 47: 1337–1342.

41. Yoshioka H, Sugie K, Park HJ, Maeda H, Tsuda N, et al. (2001) Induction of plant gp91 phox homolog by fungal cell wall, arachidonic acid, and salicylic acid in potato. Mol Plant Microbe Interact 14: 725–736.

42. Simon-Plas F, Elmayan T, Blein JP (2002) The plasma membrane oxidase NtrbohD is responsible for AOS production in elicited tobacco cells. Plant J 31: 137–147.

43. Kadota Y, Watanabe T, Fujii S, Maeda Y, Ohno R, Higashi K, Sano T, Muto S, Hasezawa S, Kuchitsu K (2005) Cell-cycle dependence of elicitor-induced signal transduction in tobacco BY-2 cells. Plant Cell Physiol 46: 156–165.

44. Torres MA, Dangl JL, Jones JD (2002) Arabidopsis gp91phox homologues AtrbohD and AtrbohF are required for accumulation of reactive oxygen intermediates in the plant defense response. Proc Natl Acad Sci U S A 99: 517–522.

45. Yoshie Y, Goto K, Takai R, Iwano M, Takayama S, et al. (2005) Function of the rice gp91phox homologs OsrbohA and OsrbohE genes in ROS-dependent plant immune responses. Plant Biotech 22: 127–135.

46. Wong HL, Pinontoan R, Hayashi K, Tabata R, Yaeno T, et al. (2007) Regulation of rice NADPH oxidase by binding of Rac GTPase to its N-terminal extension. Plant Cell 19: 4022–4034.

47. Pontier D, Tronchet M, Rogowsky P, Lam E, Roby D (1998) Activation of *hsr203*, a plant gene expressed during incompatible plant-pathogen interactions, is correlated with programmed cell death. Mol Plant Microbe Interact 11: 544–554.

48. Colcombet J, Mathieu Y, Peyronnet R, Agier N, Lelievre F, et al. (2009) R-type anion channel activation is an essential step for ROS-dependent innate immune response in Arabidopsis suspension cells. Functional Plant Biology 36: 832–843.

49. Geiger D, Scherzer S, Mumm P, Stange A, Marten I, et al. (2009) Activity of guard cell anion channel SLAC1 is controlled by drought-stress signaling kinase-phosphatase pair. Proc Natl Acad Sci U S A 106: 21425–21430.

50. Geiger D, Scherzer S, Mumm P, Marten I, Ache P, et al. (2010) Guard cell anion channel SLAC1 is regulated by CDPK protein kinases with distinct Ca^{2+} affinities. Proc Natl Acad Sci U S A 107: 8023–8028.

51. Lee SC, Lan W, Buchanan BB, Luan S (2009) A protein kinase-phosphatase pair interacts with an ion channel to regulate ABA signaling in plant guard cells. Proc Natl Acad Sci U S A 106: 21419–21424.

52. Xue S, Hu H, Ries A, Merilo E, Kollist H, et al. (2011) Central functions of bicarbonate in S-type anion channel activation and OST1 protein kinase in CO_2 signal transduction in guard cell. EMBO J 30: 1645–1658.

53. Kobayashi M, Ohura I, Kawakita K, Yokota N, Fujiwara M, et al. (2007) Calcium-dependent protein kinases regulate the production of reactive oxygen species by potato NADPH oxidase. Plant Cell 19: 1065–1080.

54. Boudsocq M, Willmann MR, McCormack M, Lee H, Shan L, et al. (2010) Differential innate immune signalling via Ca^{2+} sensor protein kinases. Nature 464: 418–422.

55. Bricchi I, Bertea CM, Occhipinti A, Paponov IA, Maffei ME (2012) Dynamics of membrane potential variation and gene expression induced by *Spodoptera littoralis*, *Myzus persicae*, and *Pseudomonas syringae* in Arabidopsis. PloS One 7: e46673.

56. Drerup M, Schlücking K, Hashimoto K, Manishankar P, Steinhorst L, et al. (2013) The calcineurin B-like calcium sensors CBL1 and CBL9 together with their interacting protein kinase CIPK26 regulate the Arabidopsis NADPH oxidase RBOHF. Mol Plant 6: 559–569.

57. Ogasawara Y, Kaya H, Hiraoka G, Yumoto F, Kimura S, et al. (2008) Synergistic Activation of Arabidopsis NADPH Oxidase AtrbohD by Ca^{2+} and Phosphorylation. J Biol Chem 283: 8885–8892.

58. Takeda S, Gapper C, Kaya H, Bell E, Kuchitsu K, et al. (2008) Local Positive Feedback Regulation Determines Cell Shape in Root Hair Cells. Science 319: 1241–1244.

59. Kimura S, Kaya H, Kawarazaki T, Hiraoka G, Senzaki E, et al. (2012) Protein phosphorylation is a prerequisite for the Ca^{2+}-dependent activation of Arabidopsis NADPH oxidases and may function as a trigger for the positive feedback regulation of Ca^{2+} and reactive oxygen species. Biochim Biophys Acta-Molecular Cell Research 1823: 398–405.

60. Jeworutzki E, Roelfsema MR, Anschütz U, Krol E, Elzenga J, et al. (2010) Early signaling through the Arabidopsis pattern recognition receptors FLS2 and EFR involves Ca^{2+}-associated opening of plasma membrane anion channels. Plant J 62: 367–378.

61. Gómez-Gómez L, Boller T (2003) Flagellin perception: a paradigm for innate immunity. Trends Plant Sci 7: 251–256.

62. Montillet JL, Leonhardt N, Mondy S, Tranchimand S, Rumeau D, et al. (2013) An abscisic acid-independent oxylipin pathway controls stomatal closure and immune defense in Arabidopsis. PLoS Biol 11: e1001513.

63. Kamoun S, Young M, Glascock CB, Tyler BM (1993) Extracellular protein elicitors from Phytophthora: host-specificity and induction of resistance to bacterial and fungal phytopathogens. Mol Plant Microbe Interact 6: 15–25.

64. Zipfel C, Robatzek S, Navarro L, Oakeley EJ, Jones JD, et al. (2004) Bacterial disease resistance in Arabidopsis through flagellin perception. Nature 428: 764–767.